Journal of Asian Earth Sciences 39 (2010) 97–108

Contents lists available at ScienceDirect

Journal of Asian Earth Sciences

journal homepage: www.elsevier.com/locate/jseaes

A precursor of the North Anatolian Fault in the Marmara Sea region

M. Zattin [a,*], W. Cavazza [b], A.I. Okay [c], I. Federici [b], M.G. Fellin [d], A. Pignalosa [b], P. Reiners [e]

[a] Dipartimento di Geoscienze, Università di Padova, Via Giotto 1, 35137 Padova, Italy
[b] Dipartimento di Scienze della Terra e Geologico-Ambientali, Università di Bologna, Piazza di Porta San Donato 1, 40126 Bologna, Italy
[c] Avrasya Yerbilimleri Enstitüsü ve Jeoloji Mühendisliği Bölümü, Maden Fakültesi, İstanbul Teknik Üniversitesi, Maslak, 34469 İstanbul, Turkey
[d] Institut für Isotopengeologie und Mineralische Rohstoffe, ETH, Clausiusstrasse 25, 8092 Zürich, Switzerland
[e] Department of Geosciences, University of Arizona, Gould-Simpson Building #77, Tucson, AZ 85721, USA

ARTICLE INFO

Article history:
Received 20 May 2009
Received in revised form 22 February 2010
Accepted 27 February 2010

Keywords:
Thermochronology
Exhumation
North Anatolian Fault
Marmara Sea

ABSTRACT

Apatite (U-Th)/He and fission-track analyses of both basement and sedimentary cover samples collected around the Marmara Sea point to the existence of a system of major E–W-trending structural discontinuities active at least from the Late Oligocene. In the Early Pliocene, inception of the present-day North Anatolian Fault (NAF) system in the Marmara region occurred by reactivation of these older tectonic structures. This is particularly evident across the Ganos fault in southern Thrace, as exhumation south of it occurred during the latest Oligocene and north of it during the mid-Miocene. In this area, large tectonic structures long interpreted as the results of Plio-Quaternary NAF-related transpressional deformation (i.e. the Ganos monocline, the Korudağ anticline, and the Gelibolu folds) were in fact produced during the Late Oligocene – Early Miocene. The overall lack of significant (U-Th)/He age differences across the NAF indicates that the Early Pliocene inception of strike–slip motion in the Marmara region represents a relatively minor episode. At the scale of the entire Marmara region, the geographic pattern of exhumation ages shown in this study results instead from the complex superposition of older tectonic events including: (i) the amalgamation of Sakarya and Anatolide–Tauride terranes and (ii) Aegean-related extension.

The Marmara Sea consists essentially of depressions and ridges aligned along the E–W trend of the North Anatolian Fault (NAF; Fig. 1). This fault system, about 1500 km long, is characterised by a right-lateral strike–slip motion and constitutes the northern boundary of the westward moving Anatolian block (e.g., Jackson and McKenzie, 1988; Barka, 1992). According to the common interpretation, the NAF nucleated in eastern Anatolia (Bitlis–Zagros suture zone) during the Late Miocene (ca. 11 Ma) following the collision of the Arabia and Eurasian plates, and propagated westward reaching the Marmara region during the Pliocene (e.g., Barka, 1992; Hubert-Ferrari et al., 2002; Şengör et al., 2005). In this region, the NAF widens into a complex fault zone stretching some 100 km in a N–S direction, from Ganos Mt. in southern Thrace (Okay et al., 2004) to Kazdağ in the southern Biga peninsula (Cavazza et al., 2008). Such configuration translates into a high degree of structural complexity, with coexisting deep basins, push-up structures, and block rotations (e.g., Seeber et al., 2004). The inception of the NAF activity has been inferred based on the study of the associated sedimentary basins, with earlier studies relying mainly on the scarce palaeontological data from terrestrial sedimentary records (see Şengör et al. (2005), for a review). The oldest basins are Middle to Late Miocene in age, whereas the youngest are hardly older than the Pleistocene. Based on apatite fission-track analysis of limited number of samples, Zattin et al. (2005) suggested that the Ganos segment of the NAF follows a pre-existing structural discontinuity in existence at least by the latest Oligocene. Late Oligocene age displacement along the NAF is also supported by Uysal et al. (2006) who studied a ca. 500 km long segment of the NAF east of the Marmara Sea by radiometric dating of fault gouges. They found that an early event of significant strike–slip was initiated at about 57 Ma, but further intensified at ~26 Ma and later than ~8 Ma. Kaymakci et al. (2007), on the basis of palaeomagnetic data, proposed that the Ganos fault and other ENE-trending faults experienced dextral strike–slip activity before the Late Pliocene development of the NAF. An Oligocene major strike–slip shear zone in western Anatolia, with an estimated right-lateral offset of 100 ± 20 km, was described also by Okay et al. (2008) in the Uludağ area, located close to the city of Bursa, about 30 km south of the Marmara Sea. All these papers support the idea that pre-existing mechanical weakness zones such as faults and shear zones greatly influence the locus of subsequent tectonic activity (e.g., Holdsworth et al., 1997).

In this paper, we build on the results by Zattin et al. (2005) to give a more complete picture of the tectonic evolution of the western NAF by using (U-Th)/He and fission-track dating on apatite.

* Corresponding author. Fax: +39 049 8272070.
E-mail address: massimiliano.zattin@unipd.it (M. Zattin).

1367-9120/$ - see front matter © 2010 Elsevier Ltd. All rights reserved.
doi:10.1016/j.jseaes.2010.02.014

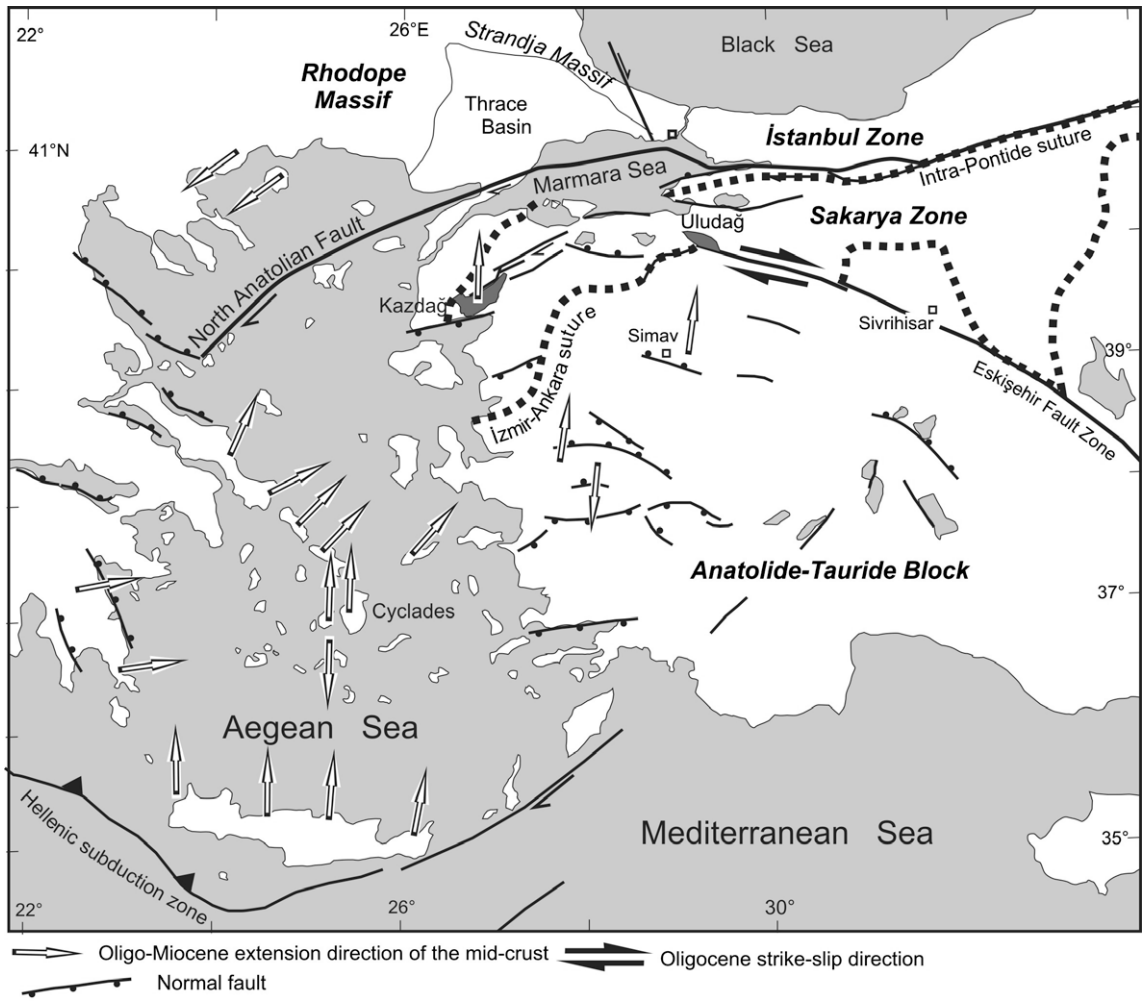

Fig. 1. Simplified tectonic map of the Marmara region showing the major terranes and sutures, as well as the North Anatolian Fault system. The large arrows refer to the direction of shear in the mid-crust during the Oligo-Miocene extension. Modified from Okay et al., 2008.

Samples were therefore collected all around the Marmara Sea and across the main strands of the fault. Our data confirm that the Marmara segments of the active NAF, regarded as post-Miocene structures, have had instead a complex evolution, as shown by the presence of pre-Late Miocene structural discontinuities along which significant vertical displacements occurred. The exact age of these earlier discontinuities is difficult to determine but should be older than the extension that affected the Aegean region since the Late Oligocene (e.g., Seyitoğlu et al., 1992; Jolivet and Faccenna, 2000). Thermochronological data by Zattin et al. (2005) demonstrate that in the Late Oligocene vertical displacements occurred along a precursor of the Ganos fault. The additional dataset presented in this paper suggests that the location and kinematics of the western NAF are controlled by position and geometry of the basement block margins inherited from Mesozoic–Cenozoic closure of oceanic basins belonging to the Tethyan realm and the ensuing collision between the bordering microcontinents.

1. Geologic setting

The Neogene tectonics of the Marmara region has been controlled by the interaction of the extensional regime driven by slab retreat along the Aegean subduction zone (e.g., Jolivet, 2001) and the westward escape of the Anatolian microplate (moving with respect to the Eurasian plate at a velocity of ~21 mm/year; e.g., Reilinger et al., 2006) guided by the NAF. In central Anatolia, over 90% of this movement is concentrated on this fault, which forms a well-defined narrow plate boundary. In the Aegean region, the rigid westward translation of the Anatolian microplate combined with back-arc spreading behind the Aegean Trench gave way to distributed north–south extension along E–W–trending normal faults. This extension resulted in the formation of E–W trending grabens, which are the most prominent neotectonic feature of western Anatolia (Bozkurt, 2001). The same structural trend is observed in the Marmara Sea region, where the NAF developed as a complex fault system. East of the Marmara Sea, the NAF splits into two branches which, divided into sub-branches, form a zone of distributed deformation more than 120 km wide (Fig. 1; Şengör et al., 1985). However, GPS studies show that over 90% of the present-day strike–slip deformation occurs along the main northern branch of NAF passing through the Marmara Sea and continuing westward into Thrace as the Ganos segment (McClusky, 2000; Meade et al., 2002). The Marmara Sea comprises a broad shelf to the south and three deep step-over sub-basins to the north (Barka, 1997; Okay et al., 2000; Le Pichon et al., 2001; Imren et al., 2001; Armijo et al., 2002). Transpressional uplift and transtensional subsidence are associated with the Ganos fault in the western Marmara region (Okay et al., 2004; Seeber et al., 2004).

The present-day tectonic framework of Anatolia is the result of a complex evolution that initiated in the Late Cretaceous with the convergence between the African and Eurasian plates. This re-

Table 1
AFT data.

Sample number	Coordinates (UTM)	Elevation (m)	No. of crystals	Spontaneous		Induced		$P(\chi)^2$	Dosimeter		Age (Ma) ± 1σ	Mean confined track length (μm) ± std err	Std. dev.	No. of tracks measured
				ρ_s	N_s	ρ_i	N_i		ρ_d	N_d				
TU1*	35T0526836 4516172	830	20	0.76	44	1.09	634	99.0	1.28	6137	16.4 ± 5.1	13.73 ± 0.23	1.64	53
TU2*	35T0524972 4515051	910	20	1.06	91	1.57	1348	89.0	1.27	6061	15.9 ± 3.4	13.50 ± 0.30	1.91	40
TU3*	35T0523523 4511909	660	20	1.17	80	1.69	1159	92.9	1.27	6022	16.1 ± 3.7	12.93 ± 0.33	1.99	37
TU4*	35T0524381 4510956	350	20	1.45	90	2.53	1565	74.2	1.26	5984	13.3 ± 2.9	14.32 ± 0.34	1.47	19
TU5*	35T0528256 4511674	1	20	2.13	104	3.86	1885	42.5	1.25	5946	11.9 ± 3.2	14.28 ± 0.17	0.76	20
TU6*	35T0508245 4501346	170	20	2.10	286	1.93	2630	94.1	1.24	5908	24.7 ± 3.1	12.60 ± 0.18	1.49	65
TU7*	35T0533648 4519168	350	20	0.67	33	1.29	640	99.9	1.24	5869	11.7 ± 4.2	14.33 ± 0.29	1.25	19
TU9*	35T0538218 4522726	120	20	1.09	74	1.55	1054	18.8	1.22	5793	15.9 ± 4.6	13.53 ± 0.38	2.03	28
TU36	35T0666467 4481129	10	12	0.49	12	0.55	134	48.1	0.95	4504	14.9 ± 5.0	–	–	–
TU38	35T0667110 4497786	200	15	3.51	193	1.16	636	20.2	0.94	4474	51.4 ± 4.8	13.43 ± 0.33	1.91	33
TU39	35T0711381 4503904	70	20	1.66	124	0.60	448	98.9	1.05	4982	53.0 ± 5.5	15.46 ± 0.11	1.07	100
TU41	35T0730648 4522849	301	20	5.83	255	1.51	661	99.9	0.94	4444	65.8 ± 5.0	13.83 ± 0.18	1.79	100
TU46	35T0274412 4495581	80	20	2.34	157	0.85	570	67.6	1.06	5021	53.3 ± 4.9	13.28 ± 0.24	1.71	52
TU47	35T0560460 4485269	25	20	2.46	199	1.44	1164	86.6	1.07	5059	33.4 ± 2.6	14.15 ± 0.15	1.04	49
TU48	35T0545966 4494013	20	20	0.51	67	0.46	597	91.6	0.94	4458	19.3 ± 2.5	14.12 ± 0.16	1.31	68
TU50	35T0549675 4495825	709	20	0.64	34	0.44	235	99.6	1.04	4924	27.5 ± 5.1	14.52 ± 0.19	1.16	38
TU51	35T0519072 4506276	310	20	2.22	103	1.69	783	37.7	0.93	4428	22.3 ± 2.5	–	–	–
TU52	35T0493388 4496841	100	30	1.44	238	1.10	1823	0.0	1.05	4963	28.3 ± 3.2	–	–	–
TU54	35T0456626 4470872	106	20	1.12	149	0.78	940	50.1	0.93	4414	27.2 ± 2.6	14.17 ± 0.16	0.96	36
TU55	35T0405489 4453934	1	14	2.91	93	1.20	385	99.6	1.10	5195	48.5 ± 5.7	–	–	–
TU56	35T0400758 4450867	250	20	2.35	275	1.66	1939	78.4	1.05	5001	27.2 ± 1.8	15.11 ± 0.10	0.98	100
TU64	35T0527608 4474219	30	8	2.81	60	1.92	410	97.7	0.93	4398	24.8 ± 3.4	–	–	–
TU92	35T0480731 4506555	350	20	1.74	139	1.37	1094	99.6	1.07	5079	24.9 ± 2.3	13.26 ± 0.33	2.08	40
TU94	35T0641940 4555239	31	14	2.71	72	1.95	517	99.9	1.05	4993	24.3 ± 3.1	13.59 ± 0.16	0.80	25
TU94	35T0662767 4556491	27	8	3.43	75	2.36	517	6.9	1.08	5122	25.6 ± 4.1	12.62 ± 0.30	1.46	23
TU96	35T0678005 4523039	1	26	1.04	137	0.71	937	84.8	1.07	508	25.4 ± 2.6	–	–	–
TU100	35T0681234 4552295	92	21	1.79	151	0.79	664	85.3	1.06	5030	39.9 ± 3.7	13.77 ± 0.232	1.20	27

Central ages calculated using dosimeter glass CN5 and ζ-CN5 = 367.45 ± 4.35 (analyst MZ) for all the samples but TU92, TU94, TU96 and TU100 (ζ-CN5 = 332.54 ± 5.55; analyst: IF). Samples marked by an asterisk (*) are from Zattin et al. (2005). ρ_s: spontaneous track densities ($\times 10^5$ cm^{-2}) measured in internal mineral surfaces; N_s: total number of spontaneous tracks; ρ_i and ρ_d: induced and dosimeter track densities ($\times 10^6$ cm^{-2}) on external mica detectors ($g = 0.5$); N_i and N_d: total numbers of tracks; $P(\chi^2)$: probability of obtaining χ^2-value for ν degrees of freedom (where ν = number of crystals-1); a probability > 5% is indicative of an homogenous population. Samples with a probability < 5% have been analysed with the binomial peak-fitting method.

sulted in the progressive closure of the Neotethyan Ocean and the amalgamation of the surrounding continental fragments. The consequent subduction–accretion complexes and emplacement of ophiolites produced the present-day crustal configuration.

In western Anatolia an extensional phase occurred during latest Oligocene–Miocene time, as testified by exhumation of the Kazdağ massif in the southern Biga Peninsula (Okay and Satir, 2000; Cavazza et al., 2008) and in the Simav complex in the northern Menderes Massif (Işık et al., 2004; Thomson and Ring, 2006). In both cases, Neogene tectonic evolution involved rapid exhumation through low-angle detachment faults followed by relative quiescence, at least in terms of vertical tectonics. The history of this extensional phase is consistent with that of the Aegean post-orogenic back-arc extension, widely recognised in the central Aegean region (e.g., Jolivet et al., 2008).

1.1. The terranes of the Marmara region

Geologically, the Marmara region resulted from the amalgamation of relatively small continental fragments: the Sakarya Zone to the south, the İstanbul Zone to the northeast and the Strandja–Rhodopian terrane cropping out all along the northern, western and southern margins of the Thrace Basin (Fig. 1; Görür and Okay, 1996; Okay and Tüysüz, 1999). According to Şengör and Yılmaz (1981), the tectonic boundary between the Sakarya and İstanbul zones – the so-called Intra-Pontide suture formed in the early Eocene after an orthogonal opening between the İstanbul and Sakarya terranes during the Liassic. Okay and Tüysüz (1999) advocated a Senonian closure of the Intra-Pontide ocean. Beccaletto et al. (2005) pointed out that the Intra-Pontide suture cannot be traced in the western Marmara region. Following is a concise description of the peri-Marmara terranes.

The Sakarya Zone is a terrane characterised by the presence of a Triassic subduction-accretion complex (Karakaya Complex), which forms a strongly deformed and partly metamorphosed basement. The final phase of deformation occurred during the latest Triassic and was followed by sedimentation of Jurassic continental to shallow-marine deposits, Cretaceous carbonates, and finally by Senonian andesites (Altıner et al., 1991; Tüysüz, 1993).

The İstanbul Zone is made of Precambrian crystalline basement overlain by a continuous transgressive sedimentary succession ranging from Ordovician to Carboniferous which was deformed during the Hercynian orogeny (Dean et al., 1997; Görür et al., 1997). The deformed Paleozoic succession is unconformably overlain by a Mesozoic succession. Senonian andesites and small acidic intrusions are widespread and are related to the northward subduction of the İzmir–Ankara ocean (Okay and Tüysüz, 1999).

The Strandja zone constitutes the easternmost part of the crystalline basement that includes the Rhodope Massif and, in the Marmara region, is made of metamorphic rocks intruded by Permian granites which are unconformably overlain by a Triassic succession (Aydın, 1974; Okay and Tüysüz, 1999). Basement and Triassic succession were regionally metamorphosed during the mid-Jurassic and then overlain by Cenomanian conglomerates and shallow marine limestones. As in the case of the İstanbul Zone, these are covered by Senonian andesites and intruded by associated granodiorites (Moore et al., 1980).

The crystalline rocks of Strandja–Rhodope represent the basement of the Thrace basin (Görür and Okay, 1996). The base of the Thrace basin fill is Early-Middle Eocene (Sakinç et al., 1999; Siyako and Huvaz, 2007) and the following deposits (until the Oligocene) form a shallowing-upward, dominantly clastic succession up to 9000-m-thick. The depocenters of the basin are characterised by locally tuffaceous siliciclastic turbidites, whereas continental to shallow-marine clastics and carbonates with subordinate volcanoclastics were laid along the margins and on elongate bathymetric highs. Dramatic lateral facies changes and the corresponding irregular subsidence patterns during the Middle Eocene (Siyako and Huvaz, 2007) have been interpreted as the result of strike–slip tectonism (e.g., Turgut et al., 1991). During the Early Oligocene, shales and sandy shales were deposited in a shelf to slope environment. Later sedimentation was characterised by coal-bearing clastics and carbonates with some tuffaceous material deposited in marginal marine to terrestrial environments (Turgut et al., 1991). During the latest Miocene–Pliocene, most of the area was characterised by fluvial deposition which lasted until the Late Pleistocene.

2. Methods

Fission-track dating is a useful tool to unravel the cooling histories experienced by rocks in the upper crustal levels and to give a measure of their motion toward the surface (for a review of the method, see Donelick et al. (2005). Fission tracks in apatites all have the same initial length of about 16 μm (the specific length depending on composition; e.g., Ketcham et al., 1999) but anneal at rates proportional to temperatures, starting from about 60 °C. Over geological time scales, partial annealing of fission tracks occurs at temperatures between about 60 and 125 °C (the Partial-Annealing Zone: PAZ; Gleadow and Fitzgerald, 1987). Because tracks shorten in relation to the degree and duration of heating, the measurement of fission track lengths gives information about the thermal evolution in the PAZ temperature range. A quantitative evaluation of the thermal history can be carried out through modelling procedures, which find a range of cooling paths compatible with the apatite fission-track (AFT) data (Ketcham, 2005). In this work, inverse modelling of track length data was performed using the HeFTy program (Ehlers et al., 2005), which generates the possible *T–t* paths by a Monte Carlo algorithm. Predicted AFT data were calculated according to the Ketcham et al. (2007) annealing model for fission tracks revelead by etching with HNO_3·5.0 N. Dpar values (i.e. the etch pit length) have been used as kinetic parameter.

The (U-Th)/He method is based on the accumulation of ^{4}He produced by the decay of ^{238}U, ^{235}U, ^{232}Th and ^{147}Sm. Radiogenic ^{4}He diffuses out of the mineral at a rate determined by the temperature and the He diffusivity of the mineral. The temperature range of the apatite He partial retention zone (PRZ) is estimated to be ~40 to 80 °C (Wolf et al., 1998). Measurements are typically made using a two-stage analytical procedure involving degassing of the crystal by heating and gas-source mass spectrometry to measure ^{4}He, followed by inductively-coupled plasma mass spectrometry on the same crystal to measure U and Th (and, in some cases, Sm). Grain ages typically have a relative standard error of approximately 3–5%, as determined by replicate measurements.

Procedures for sample preparation and analysis are outlined in Table 1 and described in more detail in Zattin et al. (2000) and Reiners (2005).

3. Analytical results

3.1. Western Marmara Sea

The westernmost samples come from Gökçeada (Fig. 2a). TU55 was collected from andesites dated at 30.4 ± 0.7 Ma (K/Ar; Ercan et al., 1995) and cutting Eocene–Oligocene flysch. The obtained AFT age (27.2 ± 1.8 Ma) and the very long track lengths (mean length = 15.11 μm; Table 1) indicate fast cooling immediately after the volcanic event. A sample from a sandstone bed of the Upper Eocene–Lower Oligocene Ceylan Fm from Gökçeada (TU54; see Gelibolu column in Fig. 3) yielded an AFT age of 48.5 ± 5.7 Ma, i.e. older

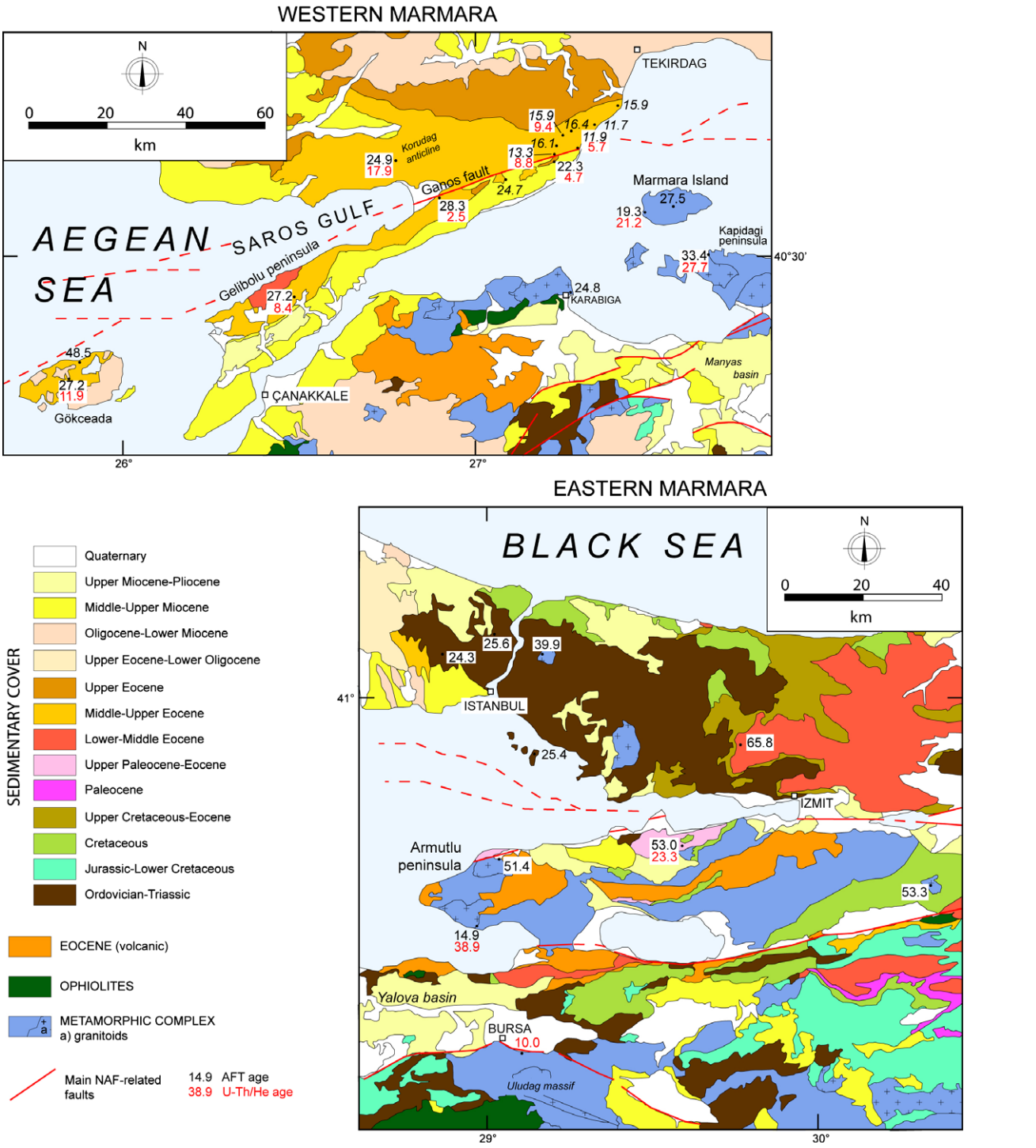

Fig. 2. Geologic map of western (A) and eastern (B) Marmara with apatite fission-track (black) and (U-Th)/He (red) ages. Fission-track data in italic are from Zattin et al., 2005.

than the depositional age considering 1σ error (Fig. 4). Given the AFT age of the andesites, we can infer that the Upper Eocene–Oligocene flysch underwent no major post-depositional burial and, therefore, the AFT age of sample TU54 is related to the cooling of the source rock and does not give any information about the post-depositional history. However, the time of exhumation of the rocks exposed on the island is constrained by AHe dating (11.9 ± 0.1 Ma, sample TU55), which indicates that: (i) the andesites were emplaced at a depth above the AHe closure temperature and (ii) final cooling took place in the Serravallian. Although the fast cooling after the volcanic event is beyond doubt, we point out that the lengths measured in sample TU55 are too long to be consistent with AHe date on same sample. This apparent discrepancy could be explained by an anomalous kinetics of fission-track annealing in these volcanic apatites.

Moving to the Gelibolu peninsula, we dated a sample (TU52) collected from a tuffite bed within the Ceylan Fm dated at 30.05 ± 0.49 Ma (Ar–Ar on biotite; Di Vincenzo, pers. comm.). Here AFT data agree with Ar–Ar data (27.2 ± 2.6 Ma), thus indicating minor post-depositional burial. Moreover, Ar–Ar and AFT data indicate that the depositional age of the Ceylan Fm reaches up the end of the Early Oligocene. Exhumation to very shallow levels occurred

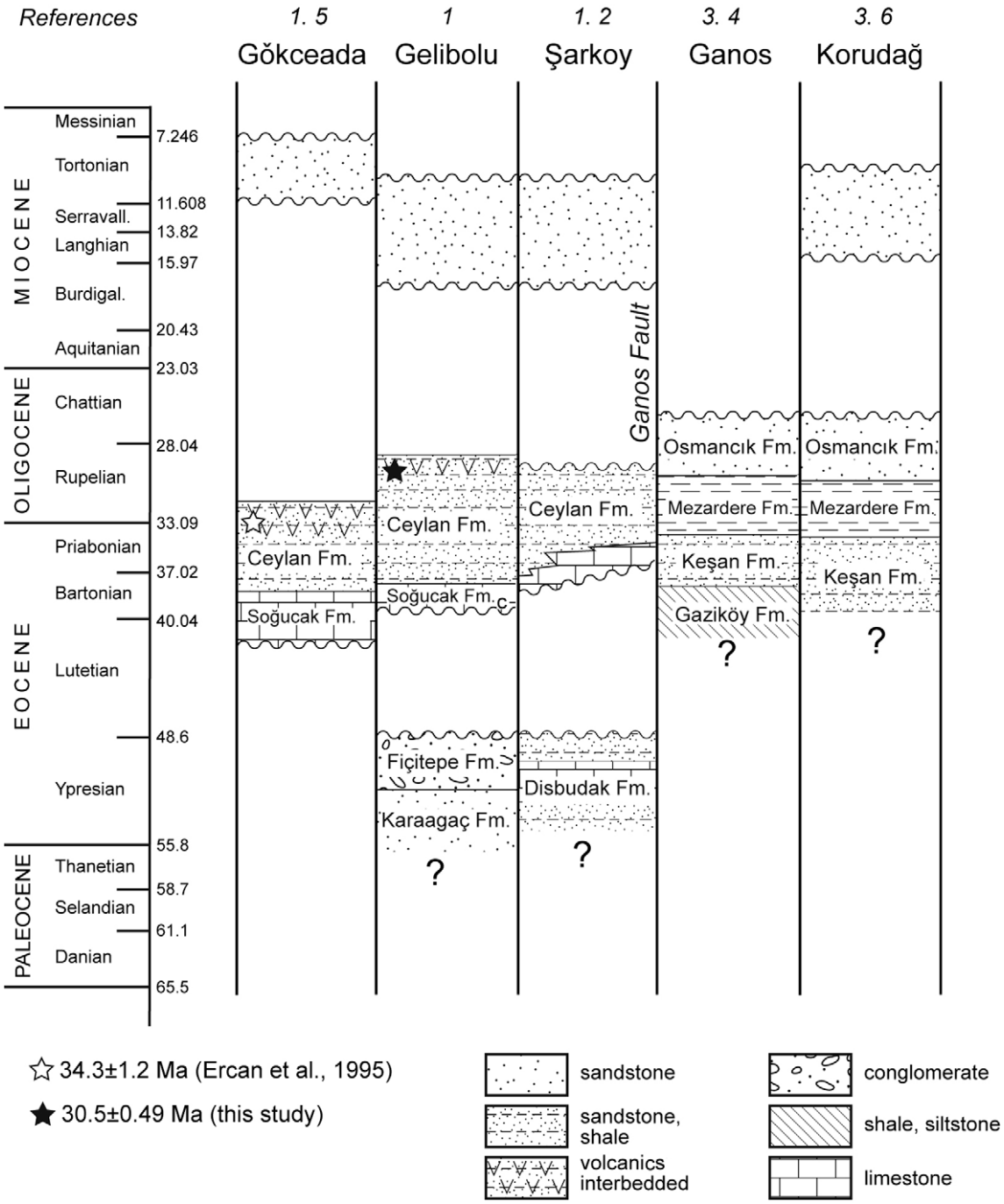

Fig. 3. Chronolitho stratigraphic chart of main lithostratigraphic units across the North Anatolian Fault in the regions from Gökceada to Ganos Mountain. Exact duration of Oligo-Miocene hiatuses north and south of Ganos fault is poorly constrained. Time scale from Gradstein et al. (2004). Sources: 1 – Özcan et al. (2010); 2 – Okay et al. (2010a,b); 3 – Sümengen and Terlemez (1991); 4 – Islamoglu et al. (2008); 5 – Ercan et al. (1995); 6 – Şentürk et al. (1998).

only in the Late Miocene, as testified by an AHe age of 8.4 ± 0.1 Ma from the same sample. The AHe age indicates some reheating that should have caused some annealing of fission tracks. Actually, the radial plot (Fig. 4) shows some grains older than depositional age that could be related to inherited apatites (i.e. not crystallized during the Oligocene magmatic event) and the younger individual grain ages could therefore be referred to some post-depositional annealing that affected the volcanic apatites. A Late Oligocene AFT exhumation age (28.3 ± 3.2 Ma) is recorded by sample TU51, collected from the Ceylan Formation (Fig. 3) exposed just south of the NAF, close to the coast of the Saros Gulf. However, here the chi-square test shows a broad dispersion of single grain ages, part of which are older than the stratigraphic age (Fig. 4). Hence, post-depositional burial was not sufficient to reset completely the fission tracks but enough to reset the AHe system which gave a very young age of 2.5 ± 0.1 Ma. Sample TU50, collected from the Keşan Formation exposed just south of the easternmost Ganos fault, gave an AFT age of 22.3 ± 2.5 Ma, slightly younger than AFT ages from previously described samples. Its AHe age is again quite young (4.7 ± 0.1 Ma).

North of sample TU51 and north of the NAF, in the core of the Korudağ anticline sample TU64 yielded an AFT age of 24.9 ± 2.3 Ma, younger than its depositional age (Eocene, Keşan Formation; Fig. 4). However, inverse modelling which was performed by using

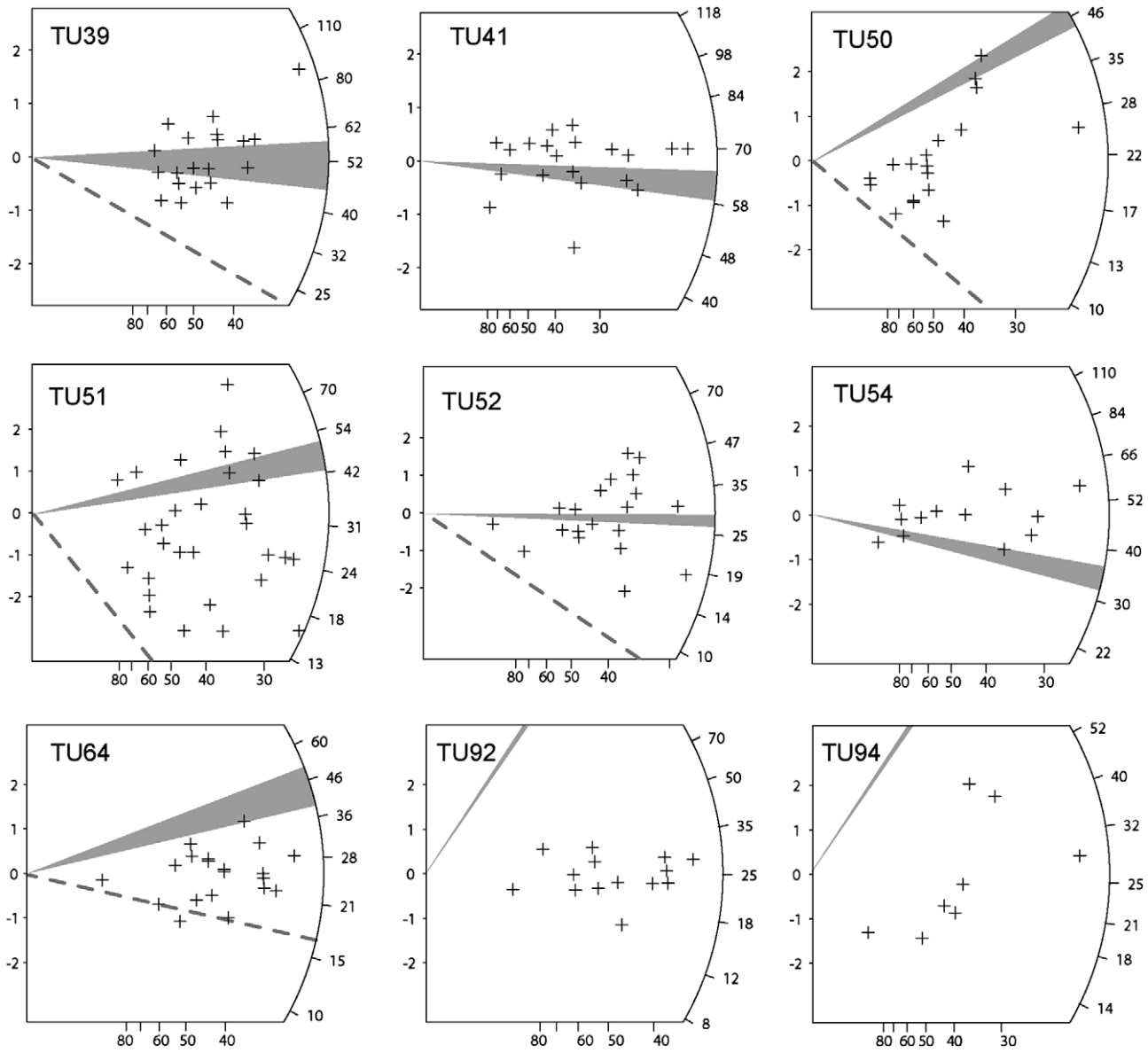

Fig. 4. Radial plots of samples collected from sedimentary rocks whose depositional age partially overlap the AFT age (see Fig. 2 for sample location). If all the single grain ages are younger than the sample's stratigraphic age, then all the grains have been annealed and maximum temperatures must have been at or greater than the total resetting temperature. As the maximum temperature lowers, the number of grain ages older the stratigraphic age generally increases. If the sample age was close to the depositional age (e.g., an ash), then partial (not only total) resetting will produce AFT ages younger than depositional age. Dots: single grain ages; horizontal axis: precision of individual grains ($1/\sigma$); vertical axis: bar indicates the standard error of each measurement; dashed line: (U-Th)/He age; shaded area: stratigraphic age.

both AFT and AHe data shows that the possible temperature range during maximum burial is quite large and comprises the bottom of the PAZ (Fig. 5). The cooling path is quite complex, and it seems to be characterised by a reduction of cooling rates in the last 15 m.y. We performed also some AHe dating on samples from the Ganos Mt. area, previously analysed with the fission-track method by Zattin et al. (2005). The oldest AHe (9.4 ± 0.1 Ma) was detected on sample TU2 collected on the top of Ganos Mountain (Table 2). This age fits well with the cooling path shown by Zattin et al. (2005) (Fig. 5). Moving towards the NAF, a slightly younger AHe age (8.8 ± 0.2 Ma) was yielded by a sample from the Gaziköy Fm (Middle Eocene; Figs. 2 and 3). The youngest age (5.7 ± 0.1 Ma) was detected on the sample closest to the NAF and at sea-level.

On the southern side of the Marmara Sea, a sample (TU56) from the Eocene Karabiga granitoids yielded an AFT age of 24.8 ± 3.4 Ma, in the same range of those obtained along the northern coast.

Two samples were taken on Marmara Island from Eocene granitoids, at sea-level (TU48) and on top of the highest peak (709 m; TU49). As expected, TU49 yielded the oldest AFT age (27.5 ± 5.1 Ma) although the age difference with the sample taken at the sea-level (19.3 ± 2.5 Ma) is quite high despite the limited elevation difference. Track lengths demonstrate that both samples cooled rapidly through the PAZ (TU48: mean length = 14.12 μm; TU49: mean length = 14.52 μm). The AHe age of sample TU48 (21.2 ± 0.5 Ma) is older than the corresponding AFT age, thus pointing to the some problems in the analytical data such as the possible presence of apatite crystals with anomalous annealing kinetics or some inclusions in the apatite dated with the AHe method.

Another sample was collected south of Marmara Island, along the western coast of the Kapıdağı peninsula (TU47). Its AFT age (33.4 ± 2.6 Ma) is significantly older than those obtained from Marmara Island and from the Eocene flysch of the Ganos area. Again,

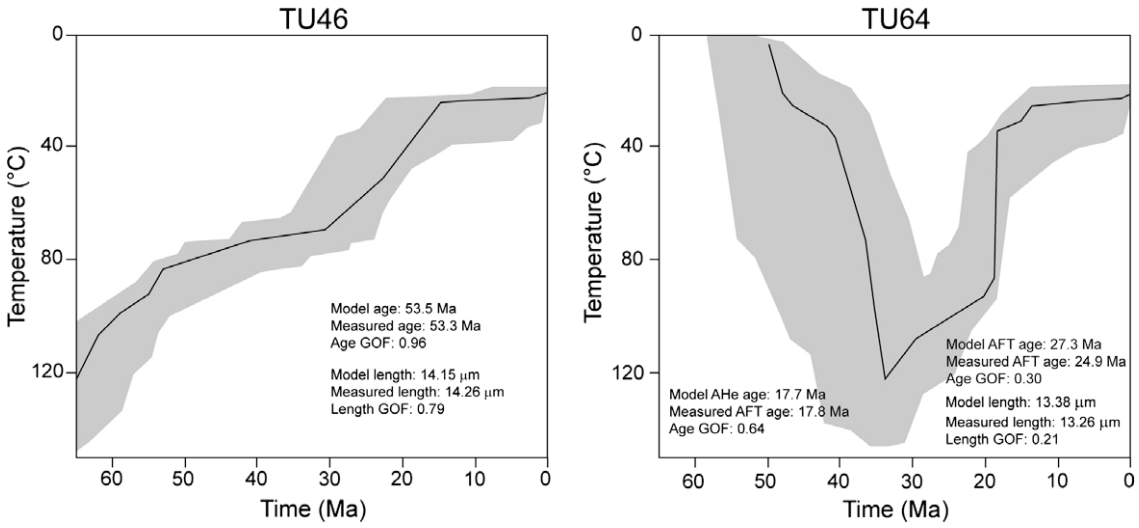

Fig. 5. Time–temperature paths obtained from inverse modelling using the HeFTy program (Ehlers et al., 2005), which generates the possible *T*–*t* paths by a Monte Carlo algorithm. Predicted AFT data were calculated according to the Ketcham et al. (2007) annealing model and the Dpar as kinetic parameter whereas AHe data were calculated according to Farley (2000) diffusion model. Shaded areas mark envelopes of statistically acceptable fit and the thick lines correspond to the most probable thermal histories. If only AFT data are modelled, thermal paths out of the partial-annealing zone are largely inferential as fission-track data cannot give reliable information out of this temperature range. In each diagram, parameters (model and measured age, model and measured mean length) related to inverse modelling are reported. GOF (Goodness-of-Fit) gives an indication about the fit between observed and predicted data (values close to 1 are best) as it reveals the probability of failing the null hypothesis that the model and data are different. In general a value of 0.05 or higher is considered not to fail the null hypothesis, and thus reflects an acceptable fit between model and data. Mean track lengths have been reported after *c*-axis projection. In these simulations, the only constraints used are the granite emplacement temperature and age (TU46) and the depositional age (TU64).

Table 2
Apatite (U-Th)/He analytical data. Refer to Table 1 for sample location.

Sample	Replicates	F_T[a]	Corrected age[b]	1σ ± (Ma)	MWAR (μm)[c]	Mass (μg)	Mean age[d]	1σ ± (Ma)
TU2	1	0.650	9.22	0.20	41.0	1.41	9.43	0.14
	2	0.700	9.61	0.18	47.5	2.14		
TU4	1	0.610	8.81	0.19	35.0	0.78	8.81	0.19
TU5	1	0.710	5.71	0.14	49.3	2.73	5.71	0.14
TU29	1	0.728	10.39	0.80	50.9	8.35	9.99	0.42
	2	0.758	9.83	0.59	56.4	10.74		
TU36	1	0.643	38.88	1.13	38.8	3.53	38.88	1.13
TU39	1	0.614	23.03	1.09	35.0	2.80	23.03	1.09
TU47	1	0.653	28.70	0.69	38.1	6.01	27.75	0.39
	2	0.670	26.35	0.71	42.9	4.04		
	3	0.728	28.04	0.62	52.3	8.14		
TU48	1	0.657	21.22	0.50	38.1	4.26	21.22	0.50
TU50	1	0.551	4.27	0.12	29.5	1.79	4.67	0.08
	2	0.618	4.95	0.10	36.1	3.59		
TU51	1	0.692	2.45	0.05	47.8	6.92	2.52	0.04
	2	0.685	2.58	0.05	45.8	3.75		
TU52	1	0.585	7.66	0.15	33.9	3.10	8.38	0.10
	2	0.651	9.58	0.19	39.6	4.56		
	3	0.696	8.33	0.17	46.9	8.48		
TU55	1	0.620	12.40	0.26	26.0	4.73	11.92	0.15
	2	0.654	10.82	0.28	21.9	5.02		
	3	0.695	12.84	0.26	30.9	7.12		
TU64	1	0.594	17.86	0.37	26.7	2.25	17.86	0.37

AHe age determination are calculate using multigrain- and, in some cases, multi-replicate aliquots; propagated analytical uncertainties are 1σ; Durango apatite measured concurrently with these analyses yielded a weighted mean age of 31.6 ± 0.48 Ma I(2σ standard error, $n = 9$).

[a] F_T is the alpha-ejection correction of Farley (2000).
[b] Alpha ejection corrected age.
[c] Mass-weighted average radius.
[d] Mean ages represent weighted means with weighted errors (1σ).

track lengths indicate a fast cooling through the PAZ (mean length = 14.15 μm), as confirmed by the AHe age of 27.7 ± 0.4 Ma.

3.2. Eastern Marmara

Samples were collected from different units across a large area (Fig. 2b). Three samples (TU38, TU39, TU46) located at the same latitude show very similar AFT ages (51–53 Ma). TU39 is from a tuffitic bed interbedded with the Eocene flysch. This sample has very long fission tracks (mean length: 15.46 μm). Given that its AFT age is very close to the depositional age (Fig. 4) we can exclude that we dated the time of exhumation. It is likely that the apatites were derived from syndepositional volcanism, and that the flysch was never buried at the bottom of the PAZ. However, the AHe age (23.0 ± 1.1 Ma) suggests some possible reheating, thus pointing to an interpretation similar to one we proposed for sample TU52,

although, as in the case of sample TU55, there is a discrepancy between the AHe age and the track lengths measured on the same sample. Samples TU38 and TU46 are both from Eocene granites. Their AFT age and track length distribution are very similar and document a moderate cooling after their intrusion. Inverse modelling (Fig. 5) suggests Early Eocene intrusion and very low cooling rates (about 1.3 °C/m.y.) in the last 40 m.y. Considering a "normal" geothermal gradient of 30 ± 5 °C/km, this translates into an exhumation rate of 0.04 ± 0.01 km/m.y.

Sample TU41 was collected NW of Izmit from the Eocene flysch. This sample yielded an AFT age (65.8 ± 5.0 Ma) older than its depositional age. We can then conclude that: (i) we dated cooling and exhumation in the sediment source area and (ii) the flysch has never been buried at the bottom of the PAZ after deposition. (Although some reset is possible, given that some grains are younger than the depositional age; Fig. 4.) Four more samples were dated in the İstanbul zone. Two of them (TU92, TU94) were collected from Carboniferous sandstones and cooled in a short time range (24–26 Ma); the same age was detected in a sample from Cretaceous andesites (TU96). Measured track lengths are not sufficient to constrain reliably the thermal history. The oldest AFT age from the İstanbul zone (39.9 ± 3.7 Ma) was obtained from a sample (TU100) collected from a granite emplaced during the Late Cretaceous.

The youngest AFT age (14.9 ± 5.0 Ma) from eastern Marmara region was obtained from a sample collected from a granitic intrusion of Eocene age in the Armutlu peninsula (TU36), although only twelve grains could be dated (no track lengths). Here some problems arise from the comparison with the AHe age (38.9 ± 1.1 Ma), much older than the AFT age. It is likely that AHe age is affected by the presence of small inclusions of zircon.

4. Discussion

The data presented here, integrated by those by Zattin et al. (2005) and Okay et al. (2008), provide the first regional picture of the thermal evolution in the last 60 m.y. of both crystalline units and sedimentary successions cropping out around the Marmara Sea. Overall, samples collected west of Marmara Island underwent a larger degree of subsidence and a much younger exhumation. Moreover, we document the presence of tectonic denudation related to fault structures which – although following the trace of the present-day NAF – were active well before its inception. Age patterns could be affected by possible deformations of isotherms due to advection and/or topography effects but these processes were probably not really effective due to the low exhumation rates and the very smooth topography, with most of the samples collected at very low elevation (the only relevant relief is Ganos mountain, as discussed below).

The oldest ages have been recorded in the eastern Marmara region. Here, AFT analyses date to the Early Eocene the exhumation of the crystalline units exposed along the Armutlu peninsula and are in the same age range of the K–Ar dating of illite from the fault rocks along the NAF (Uysal et al., 2006). These data could be related to the closure of the İzmir–Ankara oceanic domain and the ensuing collision between the Sakarya terrane to the north and the Anatolide–Tauride Block to the south (Okay and Tüysüz, 1999; Okay et al., 2001). AFT ages, including the data from the sample located just north of Izmit (TU41), may indicate the timing of the final uplift related to the end of collision. This exhumation event was followed by very little if not null subsidence and no other important uplift episodes, as testified by mean track lengths, which suggest quite a fast cooling at time of exhumation, and by the AHe ages, which document that the sampled rocks were already near the surface at the end of the Oligocene.

Low-temperature thermochronometers cannot provide evidence of Eocene tectonics in western Marmara as widespread Oligo-Miocene exhumation removed any older thermal signals. At that time, the region around the Ganos fault was exhuming, confirming the conclusions by Zattin et al. (2005). AFT age differences across the Ganos fault support the presence of a nearly E–W oriented structure that was active during the Oligocene (although horizontal displacement due to Plio-Pleistocene strike–slip must be considered when comparing ages across the fault). Rocks north and south of the fault followed markedly different *T*–*t* paths (Table 1, Figs. 2 and 3 in Zattin et al., 2005). Exhumation of the southern block across the fission-track closure isotherm took place in the latest Oligocene – earliest Miocene, while the northern block was exhumed in the mid-Miocene (16.4–11.7 Ma). Such different AFT ages and thermochronologic evolutions for samples of similar depositional age and lithology suggest that a precursor of the Ganos Fault was active by late Oligocene time. This conclusion is supported also by the local stratigraphy, as the two clusters of AFT ages north and south of the fault correspond to hiatuses in the respective sedimentary successions (Fig. 3). For example, during the late Oligocene deposition came to an end in the southernmost Thrace basin, and was followed by uplift and erosion. In contrast, the Eocene succession north of the fault was still at several kilometres depth by the late Oligocene and was exhumed above the fission-track closure isotherm (110 °C) only during the Middle Miocene, when continental to marginal-marine sandstones were being deposited south of the fault (Fig. 3).

During late Oligocene time the whole Kapıdağı–Marmara Island region was being exhumed and some exhumation occurred also in the Thrace basin (Korudağ high). This structure can be linked to the uplifting shoulders related to the formation of the graben in the Gulf of Saros and to the contemporaneous development of the Kuleli-Babaeski high in the northern Thrace basin (Çağatay et al., 1998; Coskun, 2000). Furthermore, our data along the Gelibolu peninsula match well the subsidence rate curves of Coskun (2000) who shows a maximum subsidence in the Oligocene and the inversion of the basin since 26 Ma. Siyako and Huvaz (2007) date the inversion of the basin at 20 Ma but their reconstruction was made in a depocentral area about 40 km northeast of the Ganos region.

AFT ages document that most exhumation occurred in a period during which the Aegean area was dominated by extension. During this stage, the Aegean Sea began to form and exhumation led to crustal thinning and formation of sedimentary basins in the hanging walls of detachments. Detachments are widespread in the Cyclades as well as in the northern Rhodope and western Turkey (e.g., Gautier and Brun, 1994; Dinter, 1998). This extensional phase caused erosional unroofing which is well recorded by our thermochronological data although, in the Marmara region, there is no evidence of tectonic exhumation along a discrete tectonic structure, as detected, for example, in the Kazdağ core complex to the south (Okay and Satır, 2000; Cavazza et al., 2008). However, the age differences across the Ganos fault document that some tectonic lineament(s) nearly E–W oriented were active.

Integration of our results with pre-existing data indicates that tectonic structures with the same strike of the NAF were active in the Marmara region well before its inception (from 13 to 4 Ma according to different interpretations; see Şengör et al. (2005) for a review). For example, significant Oligocene E–W-trending strike–slip shear zones in the middle crust have been documented in the granitoids of the Kapıdağı peninsula (Aksoy, 1998) and in the late Oligocene gneisses and granitoids of Uludag (Okay et al., 2008). However, movement along the precursor of the WSW–ENE-trending Ganos Fault had a significant dip–slip component (Zattin et al., 2005), given the marked AFT age difference north and south of the fault. The final collision of the Arabian and Eur-

asian plates in the mid-Miocene (Dewey et al., 1986; Robertson et al., 2007; Okay et al., 2010a) and the ensuing change of stress regime resulted in a switch of these structures (both compressional and extensional) to NAF-related faults. This relatively simplistic scenario is much complicated by extension in the Aegean domain.

While Eocene collision and Oligocene–Miocene extension generated some erosion that is well recorded by low-temperature thermochronology in all the Marmara region, the new strike–slip regime produced no major vertical displacements, as shown by the relationships between AFT ages and sample elevations along the Ganos fault (Fig. 6; Zattin et al., 2005). The increase of AHe ages with elevation confirm this evidence as we could calculate a vertical displacement in the order of 2 km at a mean cooling rate of about 10 °C/m.y. in the last 5 m.y. (i.e. an exhumation rate of about 0.3 ± 0.1 km/m.y., considering a normal geothermal gradient of 30 ± 5 °C/km). Actually, as inferred by the slope of age-elevation profile of Fig. 6, the exhumation rate from about 15 to 5 Ma was not much different (about 0.2 km/m.y.). The same value can be obtained by time elapsed to cool from AFT to AHe closure temperature. The absence of significant differences in AHe ages across the Ganos fault – at least in its easternmost sector – implies that Pliocene motion along the NAF was predominantly strike–slip. However, some vertical offset and corresponding tectonic exhumation, occurred locally due to the geometry of the fault, probably in the last 3 m.y. For example, along the westernmost sector of the Ganos fault, we found the youngest AHe age (2.5 Ma), documenting a cooling rate of about 25 °C/m.y. (corresponding to an exhumation rate of about 0.8 km/m.y. considering a geothermal gradient of 30 °C/km). Oblique slip on a non-vertical master fault, which may accommodate transtension and transpression, was described in detail by Seeber et al. (2004) for a curved segment of the Ganos fault. However, it is possible that youngest ages could be related to some late cooling due to hydrothermal activity. Although the region north of Marmara Sea is characterised by normal present-day heat flow values up to 55 mW/m^2 (Pfister et al., 1998), there is the evidence of hydrothermal mineralizations during the Pleistocene on rocks close to faults related to the NAF (Ece et al., 2008).

The last stages of exhumation testified by AHe data are confirmed by stratigraphic hiatuses that document periods of no sedimentation and/or erosion. Çağatay et al. (2006) refer the presence of an erosional unconformity dated at the base of the late Pliocene in the area of the Gulf of Saros. The same age is given by Yaltırak et al. (1998) for folding and denudation of the westernmost Gelibolu peninsula. Along the Ganos fault, no Pliocene deposits are preserved, therefore confirming the enhanced erosion detected by AHe data. These age data disagree with the notion that the folds in the Gelibolu peninsula occurred in a short period of time (<10^6 years) and, above all, that they were well eroded during the Messinian salinity crisis (Armijo et al., 1999). In fact, AHe ages along the Ganos fault are younger than the base of the Alçitepe Formation (top of the Miocene), where Armijo et al. (1999) placed the main erosional unconformity.

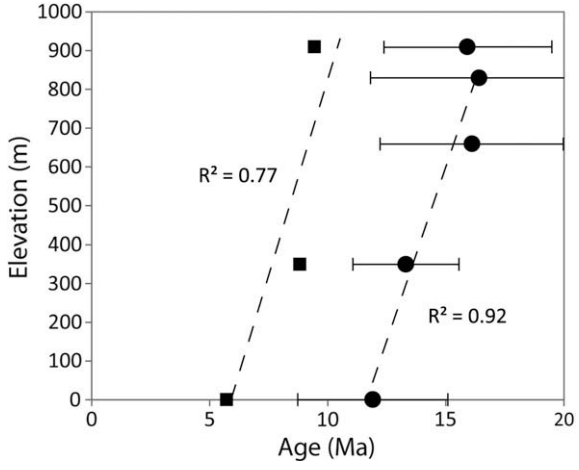

Fig. 6. Age-elevation plot for AFT (dots) and AHe (squares) data in the Ganos region. Only data from the block north of the Ganos fault have been considered. Error bars for AHe data are too small to be reported.

AHe indicate that the activity of the NAF (or a paleo-NAF) in the Armutlu peninsula produced only minor vertical displacements (i.e. total offset <1.5 km). Nonetheless exhumation was sufficient to generate an 800-m-thick fining-upward clastic sequence of Sarmatian to Lower Pliocene age (Sengör et al., 2005) in the Yalova Basin. The Manyas and Ulubat basins contain fluvial-to-lacustrine sediments whose deposition started in the late Miocene (Pontian) and continued into Early Pliocene (Yaltırak and Alpar, 2002), reaching a total thickness of about 700 m (Yalçın, 1997; Emre et al., 1998). The Mudanya basin is presently bordered on the south by the Uludağ Massif, whose exhumation was recently described by Okay et al. (2008). Here we report an AHe of 10 Ma from a sample collected at the very border of the Uludağ Massif, indicating that, in this area, a fault with a significant dip–slip component was present before the inception of the NAF.

5. Conclusions

Integration of our thermochronologic data (AFT and AHe) with pre-existing structural information (Aksoy, 1998; Okay et al., 2008) indicates that during the Oligocene E–W-trending tectonic structures were active throughout the Marmara region. Both strike–slip and dip–slip movements occurred across this wide deformation zone. Locally, these structures had significant vertical displacements and generated topographic lows and highs capable of exhuming the partial-annealing zone of apatite. For example, our data show that the present-day Ganos segment of the NAF follows the trace of a pre-existing structural discontinuity active by late Oligocene time, thus confirming the hypothesis advanced by Zattin et al. (2005). The western Marmara region south of the NAF is characterised by Late Oligocene AFT ages. We suggest that the extension that affected the region, caused by the southward migration (*rollback*) of the Aegean subduction zone, gave rise to tectonic denudation at a regional scale.

Significant vertical displacements of Neogene age are absent across most of eastern Marmara. Here thermochronological data around the Armutlu peninsula document a rapid exhumation in the Early Eocene and indicate that, at that time, all the different units were already at very shallow crustal levels. This exhumation event is probably related to the collision between the Sakarya terrane to the north and the Anatolide–Tauride Block to the south. This erosion event is recorded both in İstanbul and Sakarya terranes, thus indicating that their amalgamation occurred in pre-Eocene times (Cavazza et al., unpublished results). The NAF system in the Marmara region seems to have undergone a two-stage development dominated by: (i) dip–slip movements (both compressional and extensional) in the Oligo-Miocene and (ii) dextral strike–slip with negligible vertical movements during the Plio-Quaternary. The second stage is shown by: (i) the absence of significant AHe age differences across the main branches of the fault system, and (ii) the virtual absence of ages younger than Pliocene.

Acknowledgments

This research was sponsored by MIUR (Italian Dept. of Public Education, University and Research) and by TUBA (The Turkish

Academy of Sciences). Comments by Dr. Halim Mutlu, an anonymous reviewer and the Associate Editor Prof. Boris Natalin are gratefully acknowledged.

References

Aksoy, R., 1998. Strain Analysis of the Kapıdagı Peninsula Shear Zone in the Ocaklar Granitoid, NW Turkey. Turkish Journal of Earth Sciences 7, 79–85.

Altıner, D., Koçyiğit, A., Farinacci, A., Nicosia, U., Conti, M.A., 1991. Jurassic, Lower Cretaceous stratigraphy and paleogeographic evolution of the southern part of the northwestern Anatolia. Geologica Romana 18, 13–80.

Armijo, R., Meyer, B., Hubert, A., Barka, A., 1999. Westward propagation of the North Anatolian Fault into the northern Aegean: timing and kinematics. Geology 27, 267–270.

Armijo, R., Meyer, B., Navarro, S., King, G., 2002. Slip partitioning in the Sea of Marmara pull-apart: a clue to propagation processes of the North Anatolian Fault. Terra Nova 14, 80–86.

Aydın, Y., 1974. Etude pétrographique et géochimique de la parte centrale du Massif d'Istranca (Turquie). PhD Thesis, Université de Nancy, p. 131.

Barka, A.A., 1992. The North Anatolian Fault zone. Annales Tectonicae 6, 164–195.

Barka, A.A., 1997. Neotectonics of the Marmara region in active tectonics of Northwest Anatolia. In: Schindler, C., Pfister, M. (Eds.), The Marmara Poly-project. Hochschulverlag ETH, Zurich, pp. 55–87.

Beccaletto, L., Bartolini, A.C., Martini, R., Hochuli, P.A., Kozur, H., 2005. Biostratigraphic data from the Çetmi melange, northwest Turkey: palaeogeographic and tectonic implications. Palaeogeography, Paleoclimatology, Palaeoecology 221, 215–244.

Bozkurt, E., 2001. Neotectonics of Turkey – a synthesis. Geodinamica Acta 14, 3–30.

Çağatay, M.N., Görür, N., Alpar, B., Saatçılar, R., Akkök, R., Sakınç, M., Yüce, H., Yaltırak, C., Kuşcu, I., 1998. Geological evolution of the Gulf of Saros, NE Aegean Sea. Geo-Marine Letters 18, 1–9.

Çağatay, M.N., Görür, N., Flecker, R., Sakınç, M., Tünoglu, C., Ellam, R., Krijgsman, W., Vincent, S., Dikbas, A., 2006. Paratethyan-Mediterranean connectivity in the sea of Marmara region (NW Turkey) during the Messinian. Sedimentary Geology 188/189, 171–187.

Cavazza, W., Okay, A.I., Zattin, M., 2008. Rapid early-middle Miocene exhumation of the Kazdağ Massif. International Journal of Earth Sciences 98, 1935–1947.

Coskun, B., 2000. North Anatolian Fault–Saros Gulf relationships and their relevance to hydrocarbon exploration, northern Aegean Sea, Turkey. Marine and Petroleum Geology 17, 751–772.

Dean, W.T., Martin, F., Monod, O., Demir, O., Rickards, R.B., Bultynck, P., Bozdogan, N., 1997. Lower Paleozoic stratigraphy, Karadere–Zirze area, Central Pontides. In: Göncüoğlu, M.C., Derman, A.S. (Eds.), Early Palaeozoic Evolution in NW Gondwana, vol. 3. Turkish Association of Petroleum Geologists, pp. 32–38 (special publications).

Dewey, J.F., Hempton, M.R., Kidd, W.S.F., Şaroğlu, F., Şengör, A.M.C., 1986. Shortening of continental lithosphere: the neotectonics of Eastern Anatolia—a young collision zone. In: Coward, M.P., Ries, A.C. (Eds.), Collision Tectonics, vol. 19. Geological Society, London, pp. 3–36 (special publications).

Dinter, D.A., 1998. Late Cenozoic extension of Alpine collisional orogen, northeastern Greece. origin of the north Aegean basin. Geological Society of America Bullettin 110, 1208–1230.

Donelick, R.A., O'Sullivan, P.B., Ketcham, R.A., 2005. Apatite fission-track analysis. Review Mineralogy and Geochemistry 58, 49–94.

Ece, Ö.I., Schroeder, P.A., Smilley, M.J., Wampler, J.M., 2008. Acid–sulphate hydrothermal alteration of andesitic tuffs and genesis of halloysite and alunite deposits in the Biga Peninsula, Turkey. Clay Minerals 43, 281–315.

Ehlers, T.A., Chaudhri, T., Kumar, S., Fuller, C.W., Willett, S.D., Ketcham, R.A., Brandon, M.T., Belton, D.X., Kohn, B.P., Gleadow, A.J.W., Dunai, T.J., Fu, F.Q., 2005. Computational tools for low-temperature thermochronometer interpretation. Review Mineralogy and Geochemistry 58, 589–622.

Emre, O., Erkal, T., Tchapalyga, A., Kazancı, N., Kecer, M., Ünay, E., 1998. Neogene–Quaternary evolution of the eastern Marmara region, northwest Turkey. Bulletin of the Mineral Research and Exploration Institute of Turkey 120, 119–145.

Ercan, T., Satır, M., Steinitz, G., Dora, A., Sarifakioğlu, E., Adis, C., Walter, H.J., Yildirim, T., 1995. Biga Yarımadası ile Gokceada, Bozcaada ve Tavflan adalarındaki (KB Anadolu) Tersiyer volkanizmasının ozellikleri. Mineral Research and Exploration Institute of Turkey (MTA) Bulletin 117, 55–86.

Farley, K.A., 2000. Helium diffusion from apatite: general behavior as illustrated by Durango fluorapatite. Journal of Geophysical Research 105, 2903–2914.

Gautier, P., Brun, J.P., 1994. Ductile crust exhumation and extensional detachments in the central Aegean (Cyclades and Evvia islands). Geodinamica Acta 7, 57–85.

Gleadow, A.J.W., Fitzgerald, P.G., 1987. Uplift history and structure of the Transantarctic Mountains: new evidence from fission track dating of basement apatites in the dry valleys area, southern Victoria Land. Earth Planetary Science Letters 82, 1–14.

Görür, N., Okay, A., 1996. Origin of the Thrace basin, NW Turkey. Geologische Rundschau 85, 662–668.

Görür, N., Çağatay, M.N., Sakınç, M., Sümengen, M., Şentürk, K., Yaltirak, C., Tchapalyga, A., 1997. Origin of the Sea of Marmara as deduced from Neogene to Quaternary paleogeographic evolution of its frame. International Geology Review 39, 342–352.

Gradstein, F.M., Odd, J.G., Smith, A.G., 2004. A Geologic Time Scale 2004. Cambridge University Press, Cambridge, UK, p. 589.

Holdsworth, R.E., Butler, C.A., Roberts, A.M., 1997. The recognition of reactivation during continental deformation. Journal of Geological Society of London 154, 73–78.

Hubert-Ferrari, A., Armijo, R., King, G.C.P., Meyer, B., Barka, A., 2002. Morphology, displacement, and slip rates along the North Anatolian Fault, Turkey. Journal Geophysical Research 107, 2235.

İmren, C., Le Pichon, X., Rangin, C., Demirbğ, E., Ecevitoğlu, B., Görür, N., 2001. The North Anatolian Fault within the Sea of Marmara: a new interpretation based on multi-channel seismic and multi-beam bathymetry data. Earth Planetary Science Letters 186, 143–158.

Islamoglu, Y., Harzhauser, M., Gross, M., Jimenez-Moreno, G., Coric, S., Kroh, A., Rögl, F., van der Made, J., 2008. From Tethys to Eastern Paratethys: Oligocene depositional environments, paleoecology and paleobiogeography of the Thrace basin (NW Turkey). International Journal Earth Science 99, 183–200.

Işık, V., Tekeli, O., Seyitoğlu, G., 2004. The $^{40}Ar/^{39}Ar$ age of extensional ductile deformation and granitoid intrusion in the northern Menderes core complex: implications for the initiation of extensional tectonics in western Turkey. Journal Asian Earth Sciences 23, 555–566.

Jackson, J., McKenzie, D.P., 1988. The relationship between plate motions and seismic moment tensors, and the rates of active deformation in the Mediterranean and Middle East. Geophysical Journal 93, 45–73.

Jolivet, L., 2001. A comparison of geodetic and finite strain pattern in the Aegean, geodynamic implications. Earth Planetary Science Letters 187, 95–104.

Jolivet, L., Faccenna, C., 2000. Mediterranean extension and the Africa–Eurasia collision. Tectonics 19, 1095–1106.

Jolivet, L., Augier, R., Faccenna, C., Negro, F., Rimmele, G., Agard, P., 2008. Subduction, convergence and the mode of backarc extension in the Mediterranean region. Bulletin de la Societe Geologique de France 179, 525–550.

Kaymakci, N., Aldanmaz, E., Langereis, C., Spell, T.L., Gurer, O.F., Zanetti, K.A., 2007. Late Miocene transcurrent tectonics in NW Turkey: evidence from palaeomagnetism and $^{40}Ar–^{39}Ar$ dating of alkaline volcanic rocks. Geological Magazine 144, 379–392.

Ketcham, R.A., 2005. Forward and inverse modeling of low-temperature thermochronometry data. Reviews in Mineralogy and Geochemistry 58, 275–314.

Ketcham, R.A., Donelick, R.A., Carlson, W.D., 1999. Variability of apatite fission-track annealing kinetics III: extrapolation to geological time scales. American Mineralogist 84, 1235–1255.

Ketcham, R.A., Carter, A., Donelick, R.A., Barbarand, J., Hurford, A.J., 2007. Improved modeling of fission-track annealing in apatite. American Mineralogist 92, 799–810.

Le Pichon, X., Şengör, A.M.C., Demirbağ, E., Rangin, C., İmren, C., Armijo, R., Görür, N., Çağatay, M.N., Mercier de Lepinay, B., Meyer, B., Saatcılar, R., Tok, B., 2001. The active Main Marmara Fault. Earth and Planetary Science Letters 192, 595–616.

McClusky, S., 2000. Global Positioning System constraints on plate kinematics and dynamics in the eastern Mediterranean and Caucasus. Journal of Geophysical Research 105, 5695–5719.

Meade, B.J., Hager, B.H., McClusky, S.C., Reilinger, R.E., Ergintav, S., Onur, L., Barka, A., Özener, H., 2002. Estimates of seismic potential in the Marmara Sea region from block models of secular deformation constrained by Global Positioning System measurements. Bullettin Seismological Society of America 92, 208–215.

Moore, W.J., McKee, E.H., Akinci, Ö., 1980. Chemistry and chronology of plutonic rocks in the Pontid Mountains, northern Turkey. European Copper Deposits 1, 209–216.

Okay, A.I., Tüysüz, O., 1999. Tethyan sutures of northern Turkey. In: Durand, B., Jolivet, L., Horváth, F., Séranne, M. (Eds.), The Mediterranean Basins: Tertiary Extension within the Alpine Orogen. Geological Society, London, pp. 475–515 (special publications).

Okay, A.I., Kaşlılar-Özcan, A., İmren, C., Boztepe-Güney, A., Demirbağ, E., Kuşçu, I., 2000. Active faults and evolving strike–slip basins in the Marmara Sea, northwest Turkey: a multichannel seismic reflection study. Tectonophysics 321, 189–218.

Okay, A.I., Satır, M., 2000. Coeval plutonism and metamorphism in a latest Oligocene metamorphic core complex in northwest Turkey. Geological Magazine 137, 495–516.

Okay, A.I., Tansel, İ., Tüysüz, O., 2001. Obduction, subduction and collision as reflected in the Upper Cretaceous–Lower Eocene sedimentary record of western Turkey. Geological Magazine 138, 117–142.

Okay, A.I., Tüysüz, O., Kaya, S., 2004. From transpression to transtension: changes in morphology and structure around a bend on the North Anatolian Fault in the Marmara region. Tectonophysics 391, 259–282.

Okay, A.I., Satir, M., Zattin, M., Cavazza, W., Topuz, G., 2008. An Oligocene ductile strike–slip shear zone: the Uludag Massif, northwest Turkey – implications for the westward translation of Anatolia. Geological Society of America Bullettin 120, 893–911.

Okay, A.I., Zattin, M., Cavazza, W., 2010a. Apatite fission-track data for the Miocene Arabia–Eurasia collision. Geology 38, 35–38.

Okay, A.I., Özcan, E., Cavazza, W., Okay, N., Less, G., 2010b. Basement types, Lower Eocene series, Upper Eocene olistostromes and the initiation of the southern Thrace Basin, NW Turkey. Turkish Journal of Earth Sciences 19, 1–25.

Özcan, E., Less, L., Okay, A.I., Báldi-Beke, M., Kollányi, K., Yilmaz, İ.Ö., 2010. Stratigraphy and larger Foraminifera of the Eocene shallow-marine and olistostromal units of the southern part of the Thrace Basin, NW Turkey. Turkish Journal of Earth Sciences 19, 27–77.

Pfister, M., Rybach, L., Simsek, S., 1998. Geothermal reconaissance of the Marmara Sea region (NW Turkey): surface heat flow density in an area of active continental extension. Tectonophysics 291, 77–89.

Reilinger, R.E. et al., 2006. GPS constraints on continental deformation in the Africa–Arabia–Eurasia continental collision zone and implications for the dynamics of plate interactions. Journal of Geophysical Research 111, B05411.

Reiners, P.W., 2005. Zircon (U-Th)/He thermochronometry. Review Mineralogy and Geochemistry 58, 151–176.

Robertson, A.H.F., Parlak, O., Rızaoğlu, T., Ünlügenç, Ü., İnan, N., Tasl, K., Ustaömer, T., 2007. Tectonic evolution of the South Tethyan ocean: evidence froom the Eastern Taurus Mountains (Elaziğ region, SE Turkey). In: Ries, A.C., Butler, R.W.H., Graham, R.H. (Eds.), Deformation of continental crust, vol. 272. Geological Society of London, pp. 231–270 (special publication).

Sakinç, M., Yaltırak, C., Oktay, F.Y., 1999. Palaeogeographical evolution of the Thrace Neogene Basin and the Tethys–Paratethys relations at northwestern Turkey (Thrace). Palaeogeography, Palaeoclimatology, Palaeoecology 153, 17–40.

Seeber, L., Emre, O., Cormier, M.-H., Sorlien, C.C., McHugh, C.M.G., Polonia, A., Ozer, N., Çağatay, M.N., 2004. Uplift and subsidence from oblique slip: the Ganos–Marmara bend of the North Anatolian Transform, Western Turkey. Tectonophysics 391, 239–258.

Seyitoğlu, G., Scott, B.C., Rundle, C.C., 1992. Timing of Cenozoic extensional tectonics in west Turkey. Journal Geological Society of London 149, 533–538.

Siyako, M., Huvaz, O., 2007. Eocene stratigraphic evolution of the Thrace basin, Turkey. Sedimentary Geology 198, 75–91.

Şengör, A.M.C., Yılmaz, Y., 1981. Tethyan evolution of Turkey: a plate tectonic approach. Tectonophysics 75, 181–241.

Şengör, A.M.C., Görür, N., Şaroğlu, F., 1985. Strikeslip faulting and related basin formation in zones of tectonic escape: Turkey as a case study. In: Biddle, K.T., Christie-Blick, N. (Eds.), Strike–slip deformation basin formation and sedimentation. Society Economic Paleontology Mineralogy, pp. 227–264 (special publications).

Şengör, A.M.C., Tüysüz, O., İmren, C., Sakınç, M., Eyidoğan, H., Görür, N., Le Pichon, X., Rangin, C., 2005. The North Anatolian Fault: a new look. Annual Review Earth Planetary Science 33, 37–112.

Şentürk, K., Sümengen, M., Terlemez, I., Karaköse, C., 1998. Bandırma D-4 Sheet and 10 Page Explanatory Text, 1:100 000 Scale Geological Map Series. General Directorate of Mineral Research and Exploration, Ankara.

Sümengen, M., Terlemez, I., 1991. Stratigraphy of the Eocene sediments from the southwestern Thrace. Maden Tetkik ve Arama Dergisi 113, 17–30.

Thomson, S.N., Ring, U., 2006. Thermochronological evalution of postcollision extension in the Anatolide region, western Turkey. Tectonics 25, TC3005.

Turgut, S., Türkaslan, M., Perinçek, D., 1991. Evolution of the Thrace sedimentary basin and hydrocarbon prospectivity. In: Spencer, A.M. (Ed.), Generation, Accumulation and Production of Europe's Hydrocarbon, vol. 1. European Association of Petroleum Geosciences, pp. 415–437 (special publications).

Tüysüz, O., 1993. Karadeniz'den Orta Anadolu'ya bir jeotravers: Kuzey neo-Tetis'in tektonik evrimi. Türkiye Petrol Jeologlari Derneği Bülteni 5, 1–33.

Uysal, I.T., Mutlu, H., Altunel, E., Karabacak, V., Golding, S.D., 2006. Clay mineralogical and isotopic (K–Ar, $\delta^{18}O$, δD) constraints on the evolution of the North Anatolian Fault Zone, Turkey. Earth and Planetary Science Letters 243, 181–194.

Wolf, R.A., Farley, K.A., Kass, D.M., 1998. A sensitivity analysis of the apatite (U-Th)/He thermochronometer. Chemical Geology 148, 105–114.

Yalçın, T., 1997. Hydrogeological investigation of the Gönen and Ekşidere thermal waters (northwest Turkey). In: Schindler, C., Pfister, M. (Eds.), Active Tectonics of Northwestern Anatolia — The Marmara Poly-Project. Verlag der Fachvereine, Zürich, pp. 275–300.

Yaltırak, C., Alpar, B., Yüce, H., 1998. Tectonic elements controlling evolution of the Gulf of Saros (northeastern Aegean Sea, Turkey). Tectonophysics 300, 227–248.

Yaltırak, C., Alpar, B., 2002. Kinematics and evolution of the northern branch of the North Anatolian Fault (Ganos fault) between the Sea of Marmara and the Gulf of Saros. Marine Geology 190, 307–327.

Zattin, M., Landuzzi, A., Picotti, V., Zuffa, G.G., 2000. Discriminating between tectonic and sedimentary burial in a foredeep succession, Northern Apennines. Journal of Geological Society of London 157, 629–633.

Zattin, M., Okay, A.I., Cavazza, W., 2005. Fission-track evidence for late Oligocene and mid-Miocene activity along the North Anatolian Fault in southwestern Thrace. Terra Nova 17, 95–101.